Int. J. Heat Mass Transfer. Vol. 36, No. 4, pp. 925–930, 1993
Printed in Great Britain

0017–9310/93 $6.00 + 0.00

Superposition of thermal loads model for measuring thermal diffusivity in solids

ISAAC SHAI

The Pearlstone Center for Aeronautical Engineering Studies, Mechanical Engineering Department, Ben-Gurion University of the Negev, P.O. Box 653, Beer-Sheva 84105, Israel

and

URI LAOR and ILAN GILAD

Nuclear Research Center–Negev, P.O. Box 9001, Beer-Sheva 84190, Israel

(*Received* 13 *September* 1991 *and in final form* 1 *May* 1992)

Abstract—A new method for the measurement of the thermal diffusivity in solids using transient conditions is demonstrated. This method utilizes the principle of superposition of thermal loads. Only time measurements are required, and no accurate temperature and heat flow rate measurements are needed. The method utilizes the Seebeck effect for the measurement of the time dependence of the temperature. A solution of the heat transfer equation for the model pertinent to the described method is derived, and results obtained for several materials are presented.

INTRODUCTION

THE THERMAL conductivity of solids is an intrinsic physical property of the material, and is of great importance in determining heat flow rates and temperature distribution in the solid.

Many experimental methods for the measurement of the thermal conductivity of solids are described in the literature. Most of these methods are based on the conductive heat transfer equation solution, with well-defined boundary conditions. All of the measurements are performed by applying a thermal load to the sample, and monitoring the resulting temperature distribution in the sample. The measurements are performed under either steady state or transient conditions approximating the boundary conditions used in the analytical solution. The temperatures and heat transfer rates are measured at selected locations from which the thermal conductivity can be deduced.

In the steady-state measurements, a constant heat flux is driven through a sample of fixed cross-section. The temperatures at a few points along the sample are measured, and the thermal conductivity is calculated using Fourier's equation [1]. Other methods are performed under transient conditions [2], where the physical property measured is the thermal diffusivity rather than the thermal conductivity. Each of these methods is based on a geometrical model on which specific thermal load and boundary conditions are induced. The differential equation describing the thermal conditions is solved using the chosen boundary conditions. The solution yields a relation between the measured temperature values and the thermal diffusivity [3]. All those methods are based on accurate heat flow rate and temperature measurements using thermocouples, thermistors or infra-red detectors. The accuracy of the temperature measurements is of major importance to the accuracy of the thermal diffusivity values obtained.

Recently, a new method for the thermal diffusivity measurement in solids under transient conditions using the principle of superposition of thermal loads, has been presented [4]. In this method, an arbitrary thermal load (e.g. a continuous line source) is applied to a sample of a given shape for a time $t = t_0$. This interrupted thermal load may be treated as a superposition of a continuous line source applied at $t > 0$, together with another continuous line source of the same magnitude but of negative sign, which is applied for times $t > t_0$. The solution of the differential equation for the temperature distribution at the given thermal loads and boundary conditions shows a maximum temperature as a function of time at any point in the sample. The time at which the maximum is obtained can be accurately measured, and the accuracy of the time measurement is independent of the accuracy of the temperature measurement.

The thermoelectric effect, by which an electric EMF is built in a conductor as a result of a difference in temperature at its two ends, is instrumental as an additional means (like thermocouples, thermistors, etc.) for measuring the thermal signal.

In this paper, the above-mentioned new method for measuring the thermal diffusivity of solids is adopted. The thermal load is a one-dimensional uniform heat flux and the response signal is detected using the Seebeck effect in the sample. The ratio of the time τ, when the signal goes through a maximum, to the applied

NOMENCLATURE

C	specific heat
C_1, C_2	constants of integration
k	thermal conductivity
L	slab thickness
n	integer
q''_0	uniform heat flux
t	time
t_0	operating time of thermal load
T	temperature
T_∞	heat sink temperature
x	axial coordinate.

Greek symbols

α	thermal diffusivity, $k/\rho C$
β	parameter (equation (5))
η	parameter (equation (5))
Θ	temperature difference, $T-T_\infty$
ρ	density
τ	time to reach maximum temperature.

thermal load time t_0, relates the thermal diffusivity of the sample to its dimensions, but is independent of the Seebeck coefficient or the magnitude of the thermal disturbance.

A solution of the heat transfer equation for the model pertinent to the described method is presented. An apparatus approximating the model assumptions and using the new method, was constructed and used to measure the thermal diffusivities of several materials.

THERMAL MODEL

The thermal model chosen for the measurement of the thermal diffusivities of electrical conductors is a one-dimensional infinite slab of thickness L. One surface of the infinite slab is maintained at a constant temperature T_∞, while at the other surface a uniform heat flux is applied for a time $t = t_0$ (see Fig. 1).

Definining

$$\Theta = T - T_\infty. \tag{1}$$

The differential equation and boundary conditions for this problem are:

$$\frac{\partial^2\Theta}{\partial x^2} = \frac{1}{\alpha}\frac{\partial\Theta}{\partial t} \tag{2}$$

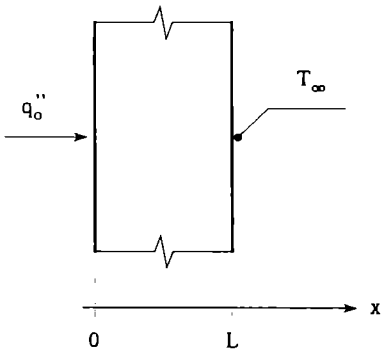

FIG. 1. The thermal model.

$$\Theta_{(x,0)} = 0 \tag{3a}$$

$$\Theta_{(L,t)} = 0 \tag{3b}$$

$$\left(\frac{\partial\Theta}{\partial x}\right)_{(0,t)} = -\frac{q''_0}{k} \quad t_0 \geqslant t > 0 \tag{3c}$$

$$\left(\frac{\partial\Theta}{\partial x}\right)_{(0,t)} = 0 \quad t > t_0. \tag{3d}$$

The detailed solution of differential equation (2) and boundary conditions (3) is given in Appendix A. The solution yields an expression for the temperature as a function of time and location in the sample, for time $t > t_0$ (see equation (A8)):

$$\Theta_{(x,t)} = \frac{8q''_0L}{\pi^2k}\left\{\sum_{n=0}^{\infty}\frac{\cos\dfrac{(2n+1)\pi x}{2L}}{(2n+1)^2}\left[e^{-(2n+1)^2\pi^2\alpha(t-t_0)/4L^2} - e^{-(2n+1)^2\pi^2\alpha t/4L^2}\right]\right\}. \tag{4}$$

Inspection of expression (4) shows that the temperature goes through a maximum at a different time for different x values. The time $t = \tau$ at which the temperature reaches a maximum is obtained by differentiating this expression with respect to time and setting the derivative to 0 (see Appendix A). Defining dimensionless parameters

$$\beta = \frac{\pi^2\alpha t_0}{4L^2}, \quad \eta = \frac{\tau}{t_0} \tag{5}$$

where the expression for β includes material properties, sample dimensions and the thermal disturbance duration. In contrast, η is the ratio of the measured time τ for the signal in the sample to reach a maximum to the applied thermal load time t_0. One obtains

$$\sum_{n=0}^{\infty}\cos\frac{(2n+1)\pi x}{2L}\left[e^{-(2n+1)^2\beta\eta} - e^{-(2n+1)^2\beta(\eta-1)}\right] = 0. \tag{6}$$

The conditions at $x = L/2$ are of special interest. It was found that truncating expression (6), after the

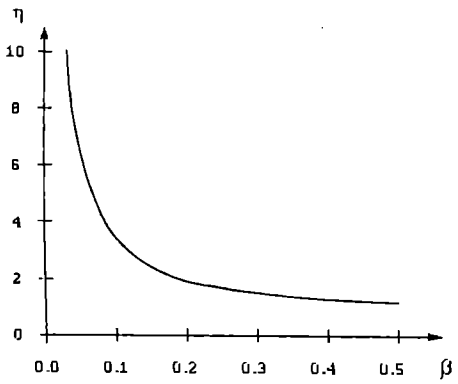

FIG. 2. η values as a function of β.

first four members, yields an inaccuracy of less than 0.001%. One obtains

$$[e^{-\beta\eta}-e^{-\beta(\eta-1)}]-[e^{-9\beta\eta}-e^{-9\beta(\eta-1)}]-[e^{-25\beta\eta}-e^{-25\beta(\eta-1)}]+[e^{-49\beta\eta}-e^{-49\beta(\eta-1)}]=0. \quad (7)$$

Rearranging expression (7) yields

$$\eta = \frac{1}{8\beta}\ln\left[\frac{(e^{9\beta}-1)+e^{-16\beta\eta}(e^{25\beta}-1)-e^{-40\beta\eta}(e^{49\beta}-1)}{e^{\beta}-1}\right]. \quad (8)$$

Equation (8) shows the relation between the measured times (appearing in η), and the material properties (in β) as shown in Fig. 2.

APPARATUS

The apparatus used for the measurements and the principle of measurement described in the present work are shown in Fig. 3.

During the measurement, the rod-shaped sample is covered by a very good insulator ($k \approx 3\times10^{-2}$ W m^{-1} C^{-1}) sleeve. This arrangement approximates the one-dimensional model used here. One end face of the sample is in good thermal contact with a cylindrical copper block which serves as a heat sink. The thermal contact is assured by applying thermal conductive paste to the copper block at the contact surface. The other end face is in contact with a very low heat capacity heater which is pressed against the rod by a spring-loaded holder. The tension of the spring can be controlled by a tightening screw. The heater is electrically insulated from the sample by a thin electrical insulator. The thermal signal from the sample is obtained via two thin copper wires touching the sample and a wire attached to the copper block. One copper wire is in contact with the sample face at the heater end, and the other at the exact center point of the sample's cylindrical face. Two thermoelectric EMFs are measured, for each copper wire with respect to the copper block which is maintained at a constant temperature. The sample and insulation are encased in a PVC housing for structural stability. The whole arrangement is constructed in a clam-shell-like formation, so that access for sample replacement and to the electrical contacts is extremely easy.

The measurement is performed by applying a constant voltage to the heater for a definite time t_0 (a square pulse heat load). The voltage to the heater, as well as the two thermoelectric EMFs obtained from the sample, are traced on a chart recorder. A representative measurement showing the obtained three curves is presented in Fig. 4. From the square heating pulse (V_H), the exact heat pulse duration t_0 is measured. The thermoelectric response (V_1) at the face of the sample which is in contact with the heater, is synchronous with the heater pulse. It starts immediately at the rise of the heater pulse, and its rise is abruptly stopped at the end of the heater pulse. On the other hand, the thermoelectric EMF at the middle of the rod (V_2) is delayed, and it rises slowly until it reaches a maximum at time τ well after the heater pulse is over.

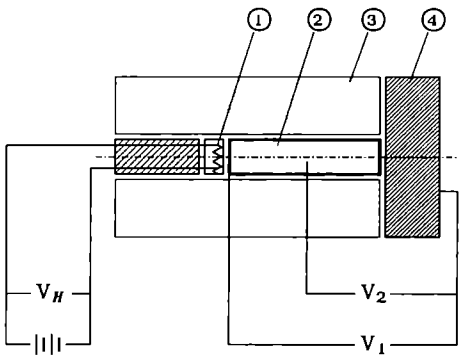

FIG. 3. Experimental apparatus and measurement principle: (1) heater; (2) sample; (3) thermal insulation; (4) heat sink (copper block).

RESULTS

The method described here utilizes the thermoelectric EMF generated by the Seebeck effect. This EMF is measured between two copper contacts with a sample on which a temperature difference is maintained. This method was used for the measurement of the thermal diffusivity of various metals. A few insulators were also measured, the measurement made possible by applying a thin Ni coating on their surfaces.

From the recorder tracings, the values of t_0 and τ were taken, β values found from equation (8) and the thermal diffusivities were calculated using equation (5). The summary of the results is shown in Table 1.

When preparing the sample and during the opti-

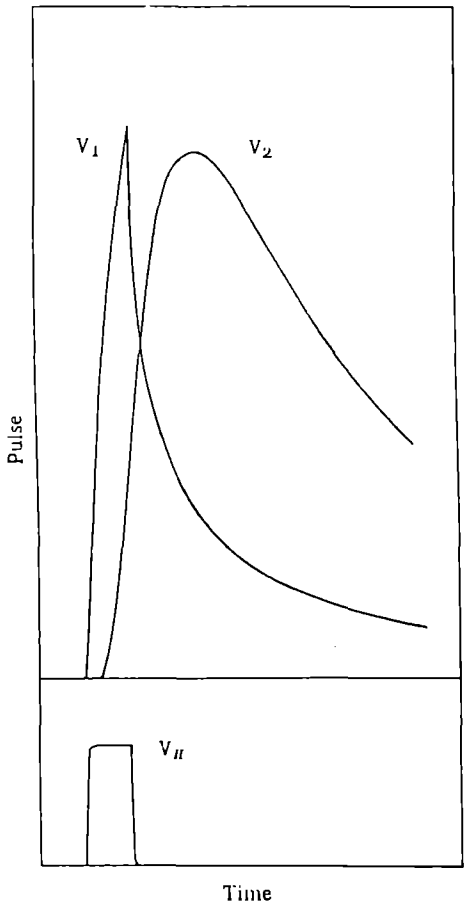

FIG. 4. Characteristic chart trace obtained for the measurement of thermal diffusivity: V_H, square voltage pulse applied to the heater; V_1, thermoelectric EMF obtained at the sample end in contact with the heater; V_2, thermoelectric EMF obtained at the midpoint of the sample.

mization of measurement parameters the following considerations had to be taken into account:

(1) The power rating of the small heater element is very limited, and therefore so is the magnitude of the thermoelectric EMF obtained for a given thermal load duration t_0 in the measurement.

(2) The thermal load duration has to be small with respect to the thermal disturbance transition time in the sample. This means that increasing the signal height by making the thermal disturbance longer is possible only up to a limit.

(3) Due to heat dissipation along the sample, the longer the sample length the weaker the obtained thermoelectric EMF signal.

(4) The ratio τ/t_0 should be in the range of 1.5–4.0, to ensure maximum sensitivity for obtaining the value of β (see Fig. 2).

The thermal disturbance transit time, τ, was measured for 3–4 different t_0 values in the sensitive range of β. Each measurement was repeated at least four times to get an estimate of result distribution and accuracy. Only one representative measurement for each material is displayed in Table 1.

DISCUSSION

All measurements in all materials were performed using different thermal disturbance durations, t_0. These values were chosen so that the $\eta = \tau/t_0$ values are obtained in the whole range of values of Fig. 2 from which β values were found (equation (8)). The thermal diffusivity values were calculated according to expression (5) for those measurements for which η values were in the range of 1.5–4.0. Measurement results for which the obtained η values were outside this range were not taken into consideration when calculating the average result and error estimation. The distribution of results obtained for measurements for a distinct η value was similar to the total distribution obtained for measurements with various η values.

Most thermal diffusivity values appearing in the literature [5] for each material are distributed over quite a wide range. One may understand this fact in one or both of the following ways: the results are accumulated from measurements performed with various methods, each of which may introduce a

Table 1. Thermal diffusivity measurements for various materials

Material	L (cm)†	t_0 (s)	τ (s)	η (—)	β (—)	α (10^{-6} m^2 s^{-1}) Present study	α (10^{-6} m^2 s^{-1}) Ref. [5]
Ti–Al–V	2.54	25.0	44.0	1.76	0.242	2.5±0.5	1.9–2.7
SS 304L	2.38	15.0	31.0	2.07	0.184	2.9±0.1	3.6
Ti	2.48	15.0	24.5	1.63	0.276	4.6±0.2	1–6
Ta	2.49	5.0	9.4	1.88	0.218	10.9±0.4	24.7‡
Nb	2.48	5.0	8.1	1.62	0.280	14±2	23.7‡
Mo	2.40	2.0	3.5	1.75	0.245	28±5	3–56
Al	2.49	2.0	3.0	1.50	0.325	41±7	86–94
Silica	2.46	60.0	118.0	1.97	0.203	0.83±0.02	1–6
Alumina	2.49	10.0	18.3	1.83	0.228	5.7±0.2	6–10

† Diameter of all samples was around 8 mm.
‡ Suggested value, by approximation, estimated in the absence of reliable results [5].

different systematic error. The thermal diffusivity of a material may depend on its constitution which is the result of composition as well as preparation procedure. There is no way to be sure about the difference in constitution between materials used in the present study and materials used in measurements cited in the literature. In the light of this comment, the agreement between results obtained in the present work and the literature is quite satisfactory.

It can be seen in Table 1 that the relative error in the measurements in aluminum and molybdenum is higher than in other materials. This larger error results from the high thermal diffusivity in those materials. The longest sample fitting into the present experimental setup limits the thermal disturbance duration, t_0, for these materials to a very short time. This, in turn, results in a weak thermoelectric signal, causing large error in the measurement of the signal maximum location. Combined with the lowered relative accuracy of time measurement for such short thermal disturbance durations, this yields a high uncertainty in the obtained results for these two materials. It remains to be seen whether constructing a longer experimental setup, which will be able to accommodate longer samples, would yield more accurate results. Certainly it would make it possible to use longer thermal disturbance durations, but the thermal dissipation along the longer sample may reduce the size of the obtained thermoelectric EMF signal back to its original magnitude. A more detailed discussion is given in Appendix B.

The measurements in insulators were performed after the deposition of a thin Ni coating. This conductive coating was required in order to obtain a thermoelectric EMF from the sample, and to close the electric circuit to enable measurements. Repeating the measurement with most of the conductive coating removed, leaving only the flat ends coated and a thin connecting strip, proved that the contribution of the coating to the thermal conductivity was negligible.

It is believed that this method can be further perfected by applying coatings made of thermoelectric materials. This would yield larger thermoelectric EMF signals, and improve measurement accuracy. The fact that the present method involves only time measurements and does not require temperature measurement, is considered to yield more accurate results than methods using temperature and power measurement.

REFERENCES

1. American National Standard, Standard method of test for thermal conductivity of materials by means of the guarded hot plate, ASTM Comm. C-16, designation C177-71. Effective October, pp. 15–28 (1971).
2. W. J. Parker, R. J. Jenkins, C. P. Butler and G. I. Abbott, Flash method of determining thermal diffusivity, heat capacity and thermal conductivity, *J. Appl. Phys.* **32**, 9 (1961).
3. H. S. Carslaw and J. C. Jaeger, *Conduction of Heat in Solids* (2nd Edn), p. 113. Oxford University Press, London (1959).
4. I. Shai, J. Aharon and I. Gilad, A quick measurement of thermal diffusivity in solids. In *Thermal Conductivity 21* (Edited by C. J. Cremers and H. A. Fine), pp. 223–231. Plenum Press, New York (1990).
5. Y. S. Touloukian (Ed.), *Thermophysical Properties of Matter, The TPRC Data Series Vol. 10: Thermal Diffusivity* (1973).

APPENDIX A. DERIVATION OF THE EQUATIONS

Uniform heat flux

The thermal model is shown schematically in Fig. 1. Defining

$$\Theta = T - T_\infty \tag{A1}$$

where T_∞ is the ambient temperature at $t = 0$ and also the constant temperature at the cold side of the sample ($x = L$), which is in good contact with the heat sink.

The differential equation and boundary conditions are

$$\frac{\partial^2\Theta}{\partial x^2} = \frac{1}{\alpha}\frac{\partial\Theta}{\partial t} \tag{A2}$$

$$\Theta_{(x,0)} = 0$$

$$\Theta_{(L,t)} = 0$$

$$\left(\frac{\partial\Theta}{\partial x}\right)_{(0,t)} = -\frac{q_0''}{k}. \tag{A3}$$

The solution for this problem is given in ref. [3]

$$\Theta_{(x,t)} = \frac{q_0''L}{k}\left[\left(1-\frac{x}{L}\right) - \frac{8}{\pi^2}\sum_{n=0}^{\infty}\frac{\cos\dfrac{(2n+1)\pi x}{2L}}{(2n+1)^2}\,e^{-(2n+1)^2\pi^2\alpha t/(4L^2)}\right] \tag{A4}$$

where $n = 0, 1, 2, 3, \ldots$. Equation (A4) shows the temperature distribution as a function of time and location in the sample.

The superposition of thermal loads

The principle of superposition of thermal loads may be applied for the solution of the problem presented above. When the thermal load in the plane $x = 0$ is given as

$$\left(\frac{\partial\Theta}{\partial x}\right)_{(0,t)} = -\frac{q_0''}{k} \quad t_0 \geqslant t > 0 \tag{A5}$$

$$\left(\frac{\partial\Theta}{\partial x}\right)_{(0,t)} = 0 \quad t > t_0. \tag{A6}$$

The principle of superposition of thermal loads may be realized by superimposing two thermal loads as shown in Fig. A1.

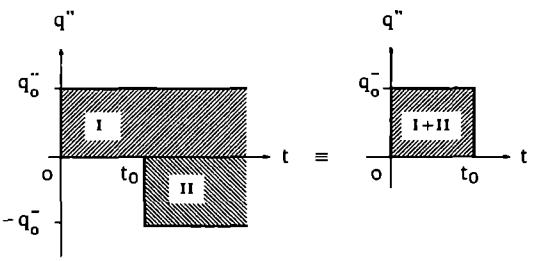

FIG. A1. The principle of superposition of thermal loads.

The resulting temperature distribution in the sample at time $t > t_0$ is the sum of the two temperature distributions obtained in expression (A4), taking into account the time lag and opposite sign of the two loads

$$\Theta_{(x,t)} = \frac{q''_0 L}{k}\left\{\left(1-\frac{x}{L}\right) - \frac{8}{\pi^2}\sum_{n=0}^{\infty}{}' \frac{\cos\dfrac{(2n+1)\pi x}{2L}}{(2n+1)^2} e^{-(2n+1)^2\pi^2\alpha t/4L^2}\right\} - \frac{q''_0 L}{k}\left\{\left(1-\frac{x}{L}\right) - \frac{8}{\pi^2}\sum_{n=0}^{\infty}{}' \frac{\cos\dfrac{(2n+1)\pi x}{2L}}{(2n+1)^2} e^{-(2n+1)^2\pi^2\alpha (t-t_0)/4L^2}\right\}. \quad \text{(A7)}$$

Rearranging the terms of this equation, one obtains

$$\Theta_{(x,t)} = \frac{8q''_0 L}{\pi^2 k}\left\{\sum_{n=0}^{\infty}{}' \frac{\cos\dfrac{(2n+1)\pi x}{2L}}{(2n+1)^2} \times \left[e^{-(2n+1)^2\pi^2\alpha(t-t_0)/4L^2} - e^{-(2n+1)^2\pi^2\alpha t/4L^2}\right]\right\}. \quad \text{(A8)}$$

APPENDIX B. ERROR ANALYSIS

In dealing with error analysis two kinds of errors should be considered. Errors which are connected to the selected model and errors which are due to the measurements.

Errors related to the model

(a) Since a very good insulation was used in the experimental test, the assumption of a one-dimensional problem is quite good.

(b) Changing the boundary condition of the model at $X = L$ from a constant temperature to a contact conductance of about $h_c = 10^4$ W m^{-2} C^{-1}, will cause an error of less than 1% in thermal diffusivity.

(c) Changing the spring tension at the heater side changes the temperature rise in the sample but does not affect the time τ.

Errors related to the measurements

(a) There is uncertainty of less than ± 0.5 mm (about $\pm 2\%$) in the location of the measuring wire at the mid-length of the sample. This can cause an error of less than $\pm 4\%$ in thermal diffusivity. When longer samples are used this error can be reduced.

(b) There might be errors in measuring the two times (t_0 and τ). The applied load time t_0 can be measured accurately; therefore a negligible error is involved with this value. The temperature–time curve at the mid-length of the sample depends on the thermoelectric signal. For metals with high Seebeck coefficient it is possible to obtain a sharp curve. When the time τ is measured from a chart, similar to the one shown in Fig. 4, then an error of about $\pm 1\%$ in η can be assumed. This will cause an error of less than $\pm 2\%$ in β (namely, in thermal diffusivity). However, by using a more accurate data acquisition system, this error can be further reduced.

In conclusion, an overall error of the order of $\pm 5\%$ can be achieved when using the presented method for measuring thermal diffusivities.